Data-based control of lightweight high-precision motion systems

Data-based control high-precision

Lightweight high-precision motion stages pose a challenge to the control design. Due to the low-frequent resonances, conventional control techniques can no longer be applied. Transfer function data, obtained from frequency response data, can be used as an extension of loop-shaping techniques. As an example it is shown how a root-locus can be drawn for an experimental set-up, without the use of a parametric model. The root-locus is then used to optimise the gain of the controller such that the settling time is minimised.

• *Rob Hoogendijk, René van de Molengraft and Maarten Steinbuch* •

The trend that the number of transistors on a chip increases while the cost of a chip decreases leads to increasing performance requirements for high-precision motion systems that are used in the chip manufacturing industry. To satisfy the specifications on the throughput and resolution, higher accelerations and improved accuracies are required. The current motion stages are designed to be very stiff to achieve the required accuracy. This makes these stages relatively heavy such that strong actuators are required. Following this design principle, increasing the accuracy would require even stiffer and consequently heavier stages. Especially for the future stages that will carry the larger 450mm wafers this will be a problem. Achieving higher accelerations with heavier stages is not feasible anymore because the high-power actuators that would be required would be inaccurate and very expensive.

Therefore, the next-generation positioning systems are designed to be lightweight to enable high accelerations using limited actuator force. At the same time, however, the system becomes less stiff causing flexible dynamics to shift to lower frequencies. Figure 1 shows typical Bode magnitude plots for a conventional system and a lightweight motion system. It can be seen that for the lightweight system resonances appear below the target bandwidth (BW). This has major consequences for the control design.

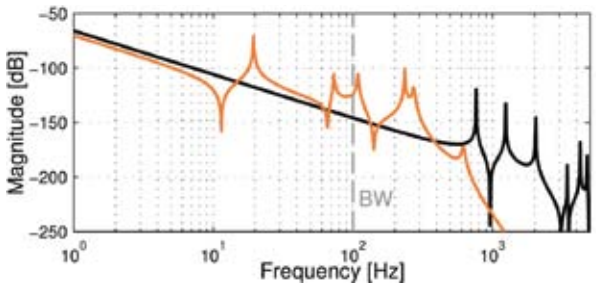

Figure 1. Typical Bode magnitude plots for a conventional high-precision motion system (black) and a lightweight motion system (orange).

# of lightweight motion systems

Rigid-body assumption

The current generation of stages is controlled in six degrees of freedom (DoFs) using multiple actuators and sensors, which makes a stage a multiple-input, multiple-output (MIMO) system. The system is decoupled by using transformation matrices in the input and output channels, such that each DoF can be controlled independently of the other DoFs. In that way, the control design of this MIMO system can be made using single-input, single-output (SISO) techniques. The computation of these transformation matrices uses the assumption that the system behaves as a rigid body. When all resonances lie above the target bandwidth, this is a valid assumption and an acceptable decoupling can be achieved. PID controllers in combination with low-pass and notch filters are used to control these systems. The notches prevent the excitation of the resonances that are present at high frequencies. Active control of these high-frequent flexible dynamics is not necessary for conventional stages, since the resonances lie well above the target bandwidth.

Advanced control

The future lightweight systems that have flexible dynamics at low frequencies cannot be decoupled by the same techniques, because they cannot be assumed to be rigid. The low-frequent resonances cause the system to display a lot of interaction between the DoFs. Furthermore, the resonances will have to be actively controlled because they lie under the target bandwidth. Therefore, advanced control techniques are required to control the future lightweight motion stages. In academia, many advanced control techniques are available, but most of them rely on an accurate model of the system. Finite-element models (FEM) are often inaccurate and computing an accurate, low-order MIMO model from frequency response measurements is also not straightforward. Therefore, the research described here focuses on data-based techniques that lie close to the loop-shaping techniques that are currently used.

Poles for performance

One of the aspects currently under investigation is how the pole locations can be computed without a model of the system. Each resonance in the Bode diagram corresponds to a complex pole pair. For a future flexible motion stage, some of these open-loop poles of the system will lie at low frequencies. Furthermore, these resonances will have a very low damping due to the use of materials with low damping such as metals and ceramics. Without proper control, the settling time of these systems would be very long. Therefore, controllers are required that can add damping to the poles to improve the settling time. Conventional loop-shaping, however, does not incorporate analysis of pole locations, since these are not known when only frequency response data of the system is available. This calls for novel control design and analysis techniques.

Experiment set-up

The techniques that have been developed will be explained by means of the experiments that were conducted on a benchmark motion system. Theory that was used will be explained along the way. The system depicted in Figure 2 consists of two inertias connected via a rotational spring. A motor is used to drive one of the inertias and the angle of

Authors' note

Rob Hoogendijk is a Ph.D. candidate at Eindhoven University of Technology, the Netherlands, in the group of Professor of Control Systems Technology, Maarten Steinbuch. His research, supervised by Associate Professor, René van de Molengraft, is part of the XTreme Motion project, which focuses on the development of high-precision positioning systems for the semiconductor industry.

This article was, in part, based on a presentation at the DSPE Conference, which was held on 4 and 5 September 2012 in Deurne, the Netherlands.

www.tue.nl

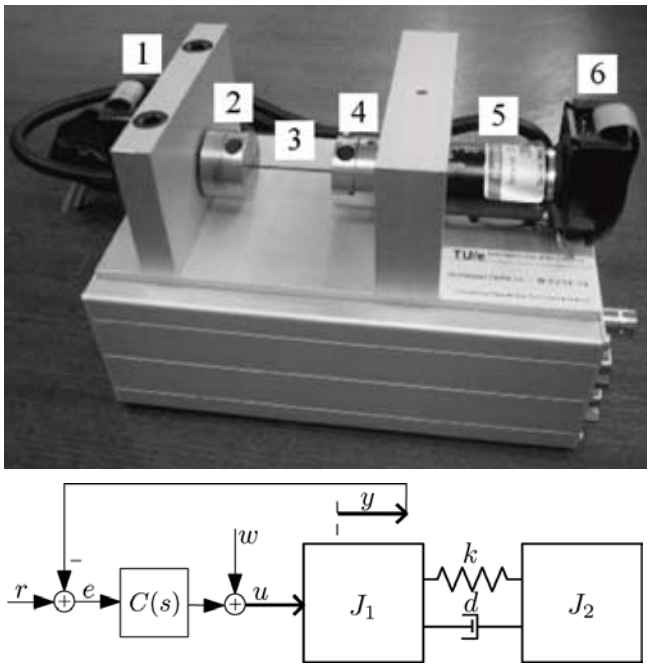

Figure 2. Top: Experimental set-up consisting of load encoder (1), load side inertia (2), rotational spring (3), motor side inertia (4), motor (5) and motor encoder (6).
Bottom: Schematic representation of the system and the feedback loop.

the inertias is measured by encoders. For this experiment, a feedback loop is closed over the motor encoder, creating a collocated control scheme as schematically depicted in the bottom part of the figure.

The feedback controller $C(s)$ consists of a gain, a lead-lag filter and a low-pas filter. The lead-lag filter creates phase lead which will add damping to the poles. Frequency response measurements have been conducted on the set-up to obtain frequency response data $H(j\omega)$. Figure 3 depicts the open-loop Bode plot of the system with controller. Three choices for the gain are shown; the low-gain case is plotted in blue, the medium-gain case in green and the high-gain case in red. But which of the open-loop transfer functions that are shown gives the best closed-loop performance? This question cannot be answered from this figure. Information on the damping of the closed-loop poles is necessary to answer this question.

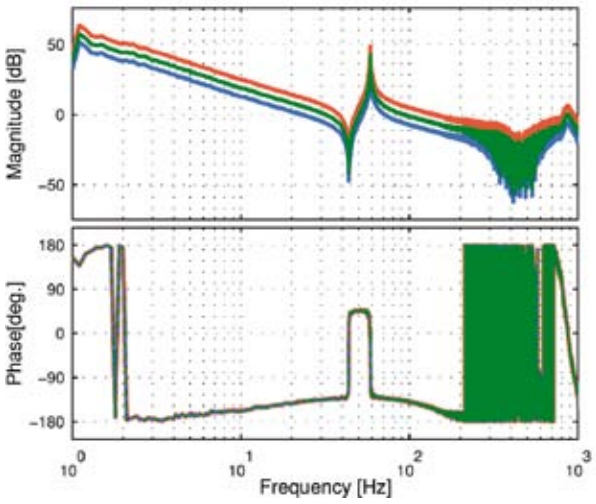

Figure 3. Bode diagram of the open loop of the experimental set-up. Three possible choices for the gain are depicted: low (blue), medium (green) and high gain (red).

Transfer function data

Closed-loop transfer functions all share the same denominator, $1+H(s)C(s)$. Consider for example the sensitivity function $S(s)$ or complementary sensitivity function $T(s)$ of a system $H(s)$ with controller $C(s)$,

$$S(s) = \frac{1}{1+H(s)C(s)}, \quad T(s) = \frac{H(s)C(s)}{1+H(s)C(s)}. \qquad (1)$$

This shows that the closed-loop poles lie at the points s where the denominator equals zero

$$p_{cl} = \{ s \mid 1+H(s)C(s) = 0 \} \qquad (2)$$

Note that at these points $H(s)C(s) = -1$, which is of course the well-known "–1 point" of the Nyquist plot. The transfer functions are denoted as a function of s and not $j\omega$, since solutions to this equation are not likely to lie on the imaginary axis. Solutions on the imaginary axis would mean that there are closed-loop poles that have zero damping, which is of course very undesirable. This means that information on $H(s)$ and not $H(j\omega)$ is required to solve this equation. This leads to the concept of transfer function data. While frequency response data $H(j\omega)$ only gives information on the transfer function $H(s)$ for points $s=j\omega$ that lie on the imaginary axis, transfer function data $H(s_i)$ gives information on the transfer function for points $s = s_i$ that can lie anywhere in the complex plane. Thus

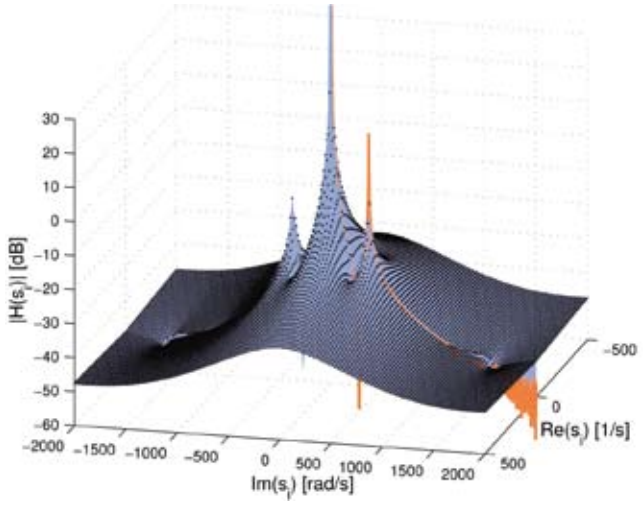

Figure 4. Transfer function data (black dots) and frequency response data (orange) of the experimental set-up.

$$s_i = \sigma_i + j\omega_i, \tag{3}$$

where σ_i denotes the damping and ω_i the frequency at this point. The subscript i emphases that s_i is a single data point in the complex plane. For lightly damped mechanical systems there is a technique to compute a point $H(s_i)$ from the measured frequency response data $H(j\omega)$ using the following Cauchy integral

$$H(s_i) = \frac{1}{2\pi} \int_{-\infty}^{\infty} \frac{H(j\omega)}{(s_i - \omega)}\, d\omega, \tag{4}$$

where s_i is a point in the right half plane. The integral (4) can only be computed for points that lie in the right half plane, because the right half plane does not contain open-loop poles. Fortunately, the systems under consideration are very lightly damped such that the open-loop poles lie almost on the imaginary axis. This makes the system symmetric in the origin such that points in the left half plane can be computed from points in the right half plane according to

$$H(s_i) = H(-s_i). \tag{5}$$

In this way it is possible to compute the value of a transfer function at any point s_i in the complex plane. More details on the computation of transfer function data can be found in [1]. By computing $H(s_i)$ on a grid of points s_i, the value of the transfer function is obtained on the whole complex plane.

Transfer function data has been computed for the experiment set-up. Figure 4 shows the 3D-Bode magnitude plot of the transfer function data of the set-up. In a 3D-Bode magnitude plot, the magnitude of the transfer function $|H(s_i)|$ is plotted as a function of both the real part σ_i and the imaginary part ω_i of s_i. The measured frequency response data is also shown in the figure in orange. Unlike the frequency response data, the transfer function data is very smooth, almost as if they were obtained from a model, which is of course not the case. This smoothness is caused by the integral (4), which has an averaging effect on measurement noise. From the figure it can also be observed that the open poles of the system (the peaks) lie on the imaginary axis, showing that the open-loop system is highly undamped such that the transfer function data is symmetric with respect to the origin of the complex plane.

Data-based root-locus

The transfer function data is obtained for the open-loop system. Next, the influence of the controller is discussed. The controller adds damping to the poles, placing the closed-loop poles somewhere in the left half plane. It is desirable to know the locations of the closed-loop poles such that the settling time and dominant frequencies in the response can be predicted. One approach is to evaluate (2) in a data-based way using the computed transfer function data of the system $H(s_i)$ and the value of the controller $C(s_i)$ yielding

$$p_{cl} = \{\, s_i \mid 1 + H(s_i)C(s_i) = 0 \,\}. \tag{6}$$

A numeric algorithm could be used to perform a search over all computed grid points s_i to look for points s_i that satisfy this equation. This would give the closed-loop poles for one specific controller. For SISO systems, however, it is even possible to compute a root-locus in a fully data-based way. The root-locus gives all possible closed-loop pole locations as a function of the gain of the controller. The controller gain k is extracted from (5) according to

$$p_{cl} = \{\, s_i \mid 1 + kH(s_i)C(s_i) = 0 \,\}. \tag{7}$$

$$p_{cl} = \{\, s_i \mid H(s_i)C(s_i) = -\frac{1}{k} \,\}. \tag{8}$$

This means that points s_i for which $H(s_i)C(s_i)$ is negative and real, belong to the root-locus. In other words, a search for points s_i where the imaginary part of $H(s_i)C(s_i)$ is zero must be performed. Moreover, the corresponding root-locus gain is given by

$$k = \frac{-1}{H(s_i)C(s_i)}, \qquad (9)$$

which immediately gives the gain of the controller that is required to achieve these closed-loop pole locations.

This computation is performed for the experimental set-up, see Figure 5. The orange and purple colour indicate the sign of the imaginary part of $H(s_i)C(s_i)$. Points that belong to the root-locus are those points where the imaginary part crosses zero *and* where the real part is negative as well. These points are indicated by the black dots. Along the lines formed by these dots, the gain of the controller goes from zero at the open-loop poles to infinity at the zeros of the plant. From the root-locus it is obvious that the optimal closed-loop pole locations are indicated by 'b', since for this choice the poles lie the farthest in the left half plane which will give the fastest settling time. At 'b' the gain k = 8.58, which is computed using (9). Apparently, there is a certain optimal gain in terms of settling time. Increasing or decreasing the gain will deteriorate the response. To show this, the closed-loop pole locations 'a' and 'c' are analysed as well. At 'a' and 'c' the gains are half and twice the value of b. Thus at 'a' k = 4.29 and at 'b' k = 17.16. These are also the three values for the gain that were shown in Figure 3, hence the corresponding colours.

Time domain response

To verify that the controller with gain k = 8.58 indeed has the best response, time domain measurements have been conducted on the set-up with all three controllers, see Figure 6. As predicted, the controller with k = 8.58 indeed has the shortest settling time. The power spectral density of the three responses is computed as well, see Figure 7. It can be seen that the dominant frequencies in the spectra correspond to the frequencies of the predicted closed-loop pole locations. The frequency is in rad/s for ease of comparison with Figure 6. The controller with k = 4.29 shows two peaks; one at 120 rad/s and one at 377 rad/s. This corresponds to the predicted locations in Figure 6, since the imaginary parts of the closed-loop poles at location 'a' have exactly those values. For k = 8.58 only

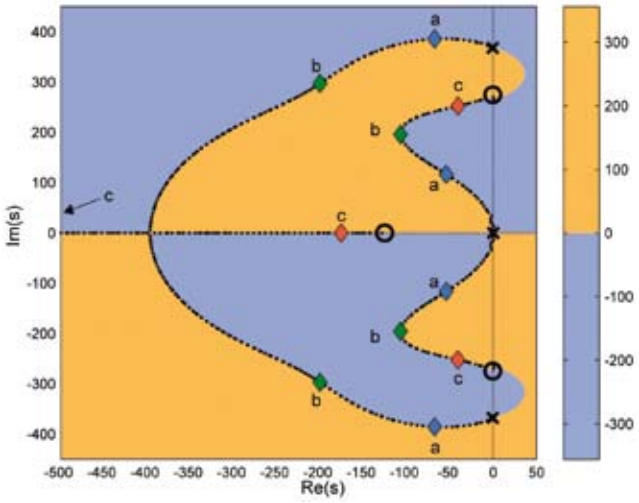

Figure 5. Root-locus computed from transfer function data. The points a, b, and c give the selected closed-loop pole locations. Open loop poles **x** and zeros **o** are indicated as well.

one peak at 207 rad/s can be distinguished in the spectrum, which corresponds to one of the two closed-loop pole pairs at 'b' in Figure 6. The second closed-loop pole pair, at 300 rad/s, is not visible in the spectrum due to its high decay rate. The same holds for k = 17.16, where the peak in the spectrum at 257 rad/s corresponds to the points 'c' in Figure 5.

While it is fairly simple to verify the frequencies of the closed-loop poles via the power spectrum, obtaining a numeric value for the real part of the pole location from the time domain response is not so straightforward. The amplitude of the response should be of the form

$$h(t) = c \cdot e^{-\sigma t} \qquad (10)$$

Where c is a constant and σ is the real part of the pole. Fitting this function on so few peaks proved to be very inaccurate. Nevertheless, when comparing the responses it can be said that it is possible to conclude that the σ value of the controller with k = 8.58 is higher than that of the other two controllers. This shows that it is possible to optimise the gain of the controller using this technique.

Conclusions

Lightweight high-precision motion stages pose a challenge to the control design of such systems. Due to the low-

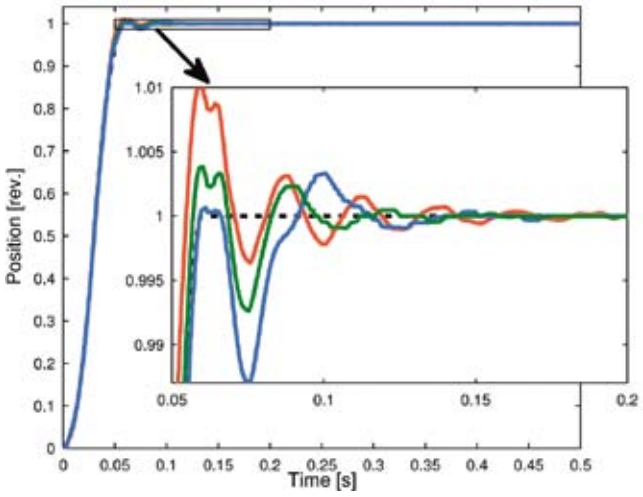

Figure 6. Time domain responses for the three selected gains; k = 4.29 (blue), k = 8.58 (green) and k = 17.16 (red).

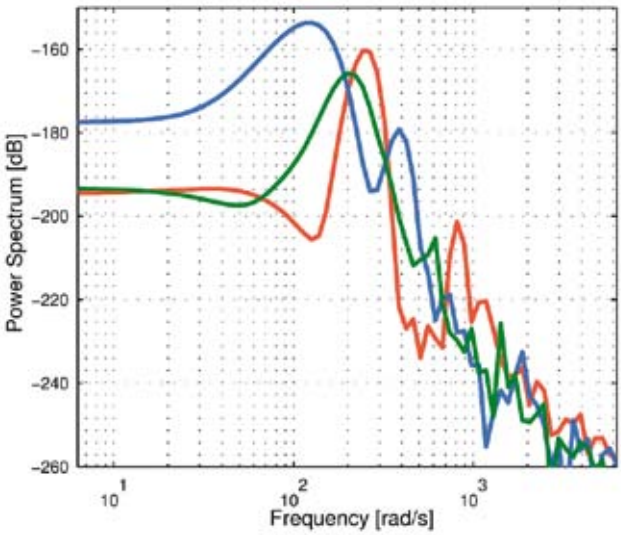

Figure 7. Power spectral density plots of the responses of Figure 6.

frequent resonances, conventional control techniques can no longer be applied. In this article it is shown that transfer function data, obtained from frequency response data, can be used as an extension of loop-shaping techniques. As an example it is shown how a root-locus can be drawn for an experimental set-up, without the use of a parametric model. The root-locus is used to optimise the gain of the controller such that the settling time is minimised. Time domain measurements on the set-up confirm the accurate prediction of the closed-loop poles.

Although the experiments shown here were conducted on a SISO system, extension to MIMO systems is straightforward. In the near future, experiments will be conducted on a 6-DoF high-precision motion system to validate the approach on a MIMO set-up.

References

[1] R. Hoogendijk, A.J. den Hamer, G.Z. Angelis, M.J.G. van de Molengraft and M. Steinbuch, “Frequency response data-based optimal control using the symmetric root-locus”, *Control Applications (CCA), 2010, IEEE International conference on*, pp. 257-262, 2010.

[2] P. Tsiotras. “The relation between the 3-d bode diagram and the root locus: insights into the connection between these classical methods”, *Control Systems Magazine, IEEE* 25(1): 88-96, 2005.